A Finite Element Method for Cracked Components of Structures

LIU Li-ming (刘立名)[a], DUAN Meng-lan (段梦兰)[b, 1], QIN Tai-yan (秦太验)[c]

LIU Yu-biao (刘玉标)[d], LIU Chun-tu (柳春图)[d] and YU Jian-xing (余建星)[a]

[a] *School of Civil Engineering, Tianjin University, Tianjin 300072, China*

[b] *Dalian University of Technology, Dalian 116024, China*

[c] *China Classification Society, Beijing 100006, China*

[d] *Institute of Mechanics, Chinese Academy of Sciences, Beijing 100080, China*

ABSTRACT

In this paper, a method is developed for determining the effective stiffness of the cracked component. The stiffness matrix of the cracked component is integrated into the global stiffness matrix of the finite element model of the global platform for the FE calculation of the structure in any environmental conditions. The stiffness matrix equation of the cracked component is derived by use of the finite variation principle and fracture mechanics. The equivalent parameters defining the element that simulates the cracked component are mathematically presented, and can be easily used for the FE calculation of large scale cracked structures together with any finite element program. The theories developed are validated by both lab tests and numerical calculations, and applied to the evaluation of crack effect on the strength of a fixed platform and a self-elevating drilling rig.

Key words: *offshore platform*; *finite element*; *crack damage*; *fracture mechanics*; *stiffness matrix*; *component*

1. Introduction

Offshore platforms are large scale steel or concrete structures. They experience various kinds of damages such as dents, corrosion pits, cracks, deformation, etc., after years of environmental impact of winds, waves, currents, soil reactions, earthquakes and ice (Duan and Liu, 1995). The safety of the structures has always been the most important issue concerned, and it depends on the assessment of the integrity of the structures, or specifically on the assessment of the damages in the structures. Ricles *et al*. (1994) experimentally investigated the residual strength of dent-damaged tubulars. The results are compared with those from finite element modeling of dented bracing conducted by ABAQUS. Liu *et al*., (2002) presented their recent advances on the evaluation on deformed legs of offshore platforms. They developed a finite element method which was experimentally and numerically verified for such analysis. Qian *et al*. (1990) studied a cantilever beam with an edge-crack and obtained the eigenfrequencies for different crack lengths and locations. The results were applied to the detection of cracks and to the investigation of dynamic behaviour of the structure. As indicated by Gudmundson (1982), who used a first order perturbation method to predict the changes in resonance frequencies of a structure resulting from cracks, notches or other geometrical changes, cracks will change the stiffness of the cracked component, influencing the strength or safety of the structure. It is shown that finite element

---

1 Corresponding author. E-mail: mlduan@ccs.org.cn

analysis is the most effective and successful method for such assessment. In general, one component is simulated by one element in the FE model of the platform. However, in comparison with the components of the platforms, the cracks in the components are very small. The cracks must be finely meshed for accurate simulation, which can not match the large size of other elements for the components that do not have any damages. To solve this problem, a finite element method is proposed in this paper to determine the effective stiffness of the cracked component. The stiffness matrix of the cracked component is integrated into the global stiffness matrix of the finite element model of the global structure for the FE calculation in any environmental conditions. The stiffness matrix equation of the cracked component is derived by use of the finite variation principle and fracture mechanics. The equivalent parameters defining the element that simulates the cracked component are mathematically presented, and can be easily used for the FE calculation of the large scale cracked structures together with any finite element program. As an application of this method, ABAQUS is used to integrate the stiffness matrix of the cracked component into the global stiffness matrix of the finite element model of a drilling rig to calculate the stresses of the platform. The results show the effect of the cracks on the strength of the rig.

2. Assumption

A beam component with a surface semi-elliptical crack is considered, and the local coordinate system as well as the basic force vectors, the position and dimension of the crack is shown in Fig. 1. The component will be taken as one beam element if it does not have any damages. For the cracked component, it is divided into three elements according to the Saint-Venant principle that the stress field is affected only in the region adjacent to the crack and the element stiffness matrix, except for the cracked element, can be regarded as unchanged under a certain limitation of element size. The middle element acts as a linear spring that does not have length and is called the damaged one, as shown in Fig. 2. The other two without any damages have a length of l_1 and l_2 respectively. The equivalent element stiffness matrix of the cracked component is obtained by integrating the stiffness matrices of such three elements by means of the static condensation method. It can be seen that the difficulty in solving the problem is the derivation of the stiffness matrix of the damaged element.
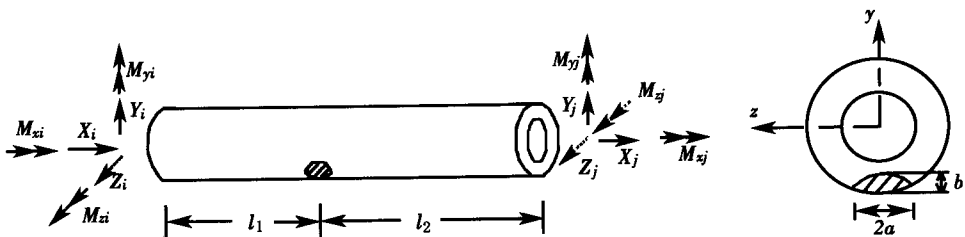

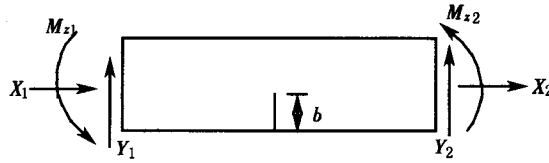**Fig. 1.** Component with a surface semi-elliptical crack.

Fig. 2. The damaged element and its sign convention.

3. FE Method for Cracked Component

3.1 Stiffness Matrix of the Damaged Element

As shown in Fig. 2, the forces at Node 1 and Node 2 present the relationship:

$$X_1 = - X_2 = X, \ Y_1 = - Y_2 = Y, \quad M_{z1} = - M_{z2} = M. \tag{1}$$

Define the difference between the corresponding displacements at the two nodes:

$$u = u_2 - u_1, \quad v = v_2 - v_1, \quad \theta_z = \theta_{z2} - \theta_{z1}. \tag{2}$$

The energy release rates G are related to the compliances λ and stress intensity factor K as presented by Irwin and Kies (1954) and Lubahn (1959):

$$\begin{cases} G_x = \dfrac{1 - \nu^2}{E}(K_{\mathrm{I}X})^2 = \dfrac{X^2}{2}\dfrac{\mathrm{d}\lambda_{uu}}{\mathrm{d}S} \\[2mm] G_y = \dfrac{1 - \nu^2}{E}(K_{\mathrm{II}Y})^2 = \dfrac{Y^2}{2}\dfrac{\mathrm{d}\lambda_{vv}}{\mathrm{d}S} \\[2mm] G_m = \dfrac{1 - \nu^2}{E}(K_{\mathrm{I}M})^2 = \dfrac{X^2}{2}\dfrac{\mathrm{d}\lambda_{\theta\theta}}{\mathrm{d}S} \end{cases} \tag{3}$$

where the compliances λ for extension, bending, and shear are defined by:

$$\begin{cases} \lambda_{uu} = \delta/X \\ \lambda_{\theta\theta} = \theta/M \\ \lambda_{vv} = w/Y \end{cases} \tag{4}$$

in which δ is axial extension, θ is rotation, and w is deflection respectively by axial load X, moment M, and shear force Y.

For Fig. 2, the correlation between the nodal forces and displacemnets is expressed as follows:

$$\begin{cases} u = \lambda_{uu}X_2 + \lambda_{u\theta}M_{z2} \\ \theta_z = \lambda_{u\theta}X_2 + \lambda_{\theta\theta}M_{z2} \\ v = \lambda_{vv}Y_2 \end{cases} \tag{5}$$

where,

$$\lambda_{uu} = \frac{2(1 - \nu^2)}{E}\int_0^S\left(\frac{K_{\mathrm{I}X}}{X}\right)^2\mathrm{d}S, \quad \lambda_{u\theta} = \frac{2(1 - \nu^2)}{E}\int_0^S\frac{K_{\mathrm{I}X}}{X}\cdot\frac{K_{\mathrm{I}M}}{M}\mathrm{d}S,$$

$$\lambda_{\theta\theta} = \frac{2(1 - \nu^2)}{E}\int_0^S\left(\frac{K_{\mathrm{I}M}}{M}\right)^2\mathrm{d}S, \quad \lambda_{vv} = \frac{2(1 - \nu^2)}{E}\int_0^S\left(\frac{K_{\mathrm{II}Y}}{Y}\right)^2\mathrm{d}S,$$

are derived from Eq.(3), E and ν are Young's modulus and Poisson's ratio respectively, S is the

area of the crack surface, and K_{IX}, $K_{\parallel Y}$, and K_{IM} stand for the stress intensity factors induced by X, Y, and M, respectively. As we know, the stress intensity factors along the edge of the crack are different. The maximum stress intensity factor at the deepest point of the crack is taken for calculating K_{IX}, $K_{\parallel Y}$, and K_{IM}.

The stress intensity factors are expressed as:

$$K_I = \frac{M_N \sigma_N + M_B \sigma_B}{E(k)} \sqrt{\pi b}, \qquad K_{\parallel} = \frac{M_Q \tau_Q}{E(k)} \sqrt{\pi b} \qquad (6)$$

where, b is the depth of the crack; M_N, M_B, and M_Q are tension, bending and shear stress correction factors defined by parameters a (length of the crack), b, t (wall thickness), and D (outer diameter); σ_N, σ_B, and τ_Q are stresses respectively induced by X_2, M_{x2}, and Y_2 when no crack exists in the element; $E(k)$ is the elliptic integral:

$$\sigma_N = \frac{X_2}{A}, \qquad \sigma_B = \frac{M_{x2} D}{2I}, \qquad \tau_Q = \frac{Y_2 S_z^*}{I},$$

$$E(k) \cong \left[1 + 1.464 \left(\frac{b}{a} \right)^{1.65} \right]^{\frac{1}{2}} \qquad k = \frac{b}{a} \leqslant 1$$

in which A, I, and S_z^* are the cross-sectional area, axial moment of inertia, and static moment about the z axis, respectively. The stress correction factors M_N and M_B are expressed as:

$$M_N = f_N(\xi, \beta) g_N(\xi) E(k);$$
$$M_B = f_B(\xi, \beta) g_B(\xi) E(k);$$

where $\xi = \dfrac{b}{t}$; $\beta = \dfrac{b}{a}$;

$$\begin{aligned}
f_N(\xi, \beta) =\ & 0.9885 + 0.1136\beta + 0.9388\beta^2 - 14.050\beta^3 \\
& + \xi(-0.0433 - 8.3171\beta + 31.698\beta^2 + 8.2269\beta^3) \\
& + \xi^2(0.9488 - 5.924\beta - 25.887\beta^2 + 4.1516\beta^3) \\
& + \xi^3(-2.4107 + 17.518\beta - 13.688\beta^2 + 5.9439\beta^3);
\end{aligned}$$

$$\begin{aligned}
f_B(\xi, \beta) =\ & 0.9730 + 0.1035\beta - 0.5642\beta^2 - 7.9135\beta^3 \\
& + \xi(0.0799 - 7.5001\beta + 38.220\beta^2 - 26.094\beta^3) \\
& + \xi^2(0.710 - 12.924\beta - 24.232\beta^2 + 55.528\beta^3) \\
& + \xi^3(-2.381 + 24.60\beta - 22.086\beta^2 - 17.262\beta^3);
\end{aligned}$$

$$\begin{aligned}
g_N(\xi) =\ & 1.1216 + 6.520\xi^2 - 12.388\xi^4 + 89.055\xi^6 \\
& - 188.608\xi^8 + 207.387\xi^{10} - 32.052\xi^{12};
\end{aligned}$$

$$\begin{aligned}
g_B(\xi) =\ & 1.1202 - 1.8872\xi - 18.014\xi^2 - 87.385\xi^3 \\
& + 241.912\xi^4 - 319.940\xi^5 + 168.011\xi^6.
\end{aligned}$$

Eq. (5) can be rewritten as

$$\begin{cases}
X = (\lambda_{\theta\theta} u - \lambda_{u\theta} \theta_z) / (\lambda_{uu} \lambda_{\theta\theta} - \lambda_{u\theta}^2) \\
M = (-\lambda_{u\theta} u + \lambda_{uu} \theta_z) / (\lambda_{uu} \lambda_{\theta\theta} - \lambda_{u\theta}^2) \\
Y = v / \lambda_{vv}
\end{cases} \qquad (7)$$

From the theory of elasticity, the strain energy U of the element is expressed as:

$$U = \frac{uX}{2} + \frac{\theta_z M}{2} + \frac{vY}{2} \tag{8}$$

which, after combination with Eq.(7), becomes

$$U = \frac{u^2 \lambda_{\theta\theta} - 2u\theta_z \lambda_{u\theta} + \theta_z^2 \lambda_{uu}}{2\Delta} + \frac{v^2}{2\lambda_{vv}} \tag{9}$$

where $\Delta = \lambda_{uu}\lambda_{\theta\theta} - \lambda_{u\theta}^2$.

Substituting Eq.(2) into Eq.(9) and minimizing the strain energy U by partial differentiation method, we obtain the stiffness equation of the damaged element with a surface semi-elliptical crack:

$$\begin{bmatrix} \dfrac{\lambda_{\theta\theta}}{\Delta} & 0 & -\dfrac{\lambda_{u\theta}}{\Delta} & -\dfrac{\lambda_{\theta\theta}}{\Delta} & 0 & \dfrac{\lambda_{u\theta}}{\Delta} \\[2mm] 0 & \dfrac{1}{\lambda_{vv}} & 0 & 0 & -\dfrac{1}{\lambda_{vv}} & 0 \\[2mm] -\dfrac{\lambda_{u\theta}}{\Delta} & 0 & \dfrac{\lambda_{uu}}{\Delta} & \dfrac{\lambda_{u\theta}}{\Delta} & 0 & -\dfrac{\lambda_{uu}}{\Delta} \\[2mm] -\dfrac{\lambda_{\theta\theta}}{\Delta} & 0 & \dfrac{\lambda_{u\theta}}{\Delta} & \dfrac{\lambda_{\theta\theta}}{\Delta} & 0 & -\dfrac{\lambda_{u\theta}}{\Delta} \\[2mm] 0 & -\dfrac{1}{\lambda_{vv}} & 0 & 0 & \dfrac{1}{\lambda_{vv}} & 0 \\[2mm] \dfrac{\lambda_{u\theta}}{\Delta} & 0 & -\dfrac{\lambda_{uu}}{\Delta} & -\dfrac{\lambda_{u\theta}}{\Delta} & 0 & \dfrac{\lambda_{uu}}{\Delta} \end{bmatrix} \begin{Bmatrix} u_1 \\ v_1 \\ \theta_{z1} \\ u_2 \\ v_2 \\ \theta_{z2} \end{Bmatrix} = \begin{Bmatrix} X_1 \\ Y_1 \\ M_{z1} \\ X_2 \\ Y_2 \\ M_{z2} \end{Bmatrix} \tag{10}$$

In consideration of the fact that the crack makes little contribution to the stresses or displacements of the element when the element is in torsion or bending on the xz plane, the discontinuation of the torsion displacements in the x and y directions as well as the displacement in the z direction on the crack surface can be ignored, i.e., $\theta_{x1} = \theta_{x2}$, $w_1 = w_2$, and $\theta_{y1} = \theta_{y2}$.

3.2 Equivalent Stiffness Matrix of the Damaged Element

The static condensation method is used to integrate the stiffness matrices of the three elements as mentioned above into the equivalent element stiffness matrix of the cracked component.

As shown in Fig. 1, the boundary nodal displacement vector can be represented by $\{U_a\} = \{u_i, v_i, w_i, \theta_{xi}, \theta_{yi}, \theta_{zi}, u_j, v_j, w_j, \theta_{xj}, \theta_{yj}, \theta_{zj}\}^T$ and the boundary nodal load vector by $\{F_a\} = \{X_i, Y_i, Z_i, M_{xi}, M_{yi}, M_{zi}, X_j, Y_j, Z_j, M_{xj}, M_{yj}, M_{zj}\}^T$. The nodal displacement vector of the damaged element, i.e., the internal nodal displacement vector of the cracked component, is taken as $\{U_b\}$, then, the stiffness equation for the cracked component can be expressed as:

$$\begin{bmatrix} K_{aa} & K_{ab} \\ K_{ba} & K_{bb} \end{bmatrix} \begin{bmatrix} U_a \\ U_b \end{bmatrix} = \begin{Bmatrix} F_a \\ 0 \end{Bmatrix}, \tag{11}$$

Eliminating the internal nodal displacement vector $\{U_b\}$ gives

$$[\overline{K}]\{U_a\} = \{F_a\}, \tag{12}$$

where $[\overline{K}]$ is the equivalent stiffness matrix of the cracked component in the local coordinate system as

shown in Fig. 1:

$$[\overline{K}] = [K_{aa}] - [K_{ab}][K_{bb}]^{-1}[K_{ba}].\tag{13}$$

3.3 Equivalent Parameters of the Cracked Component

The equivalent parameters such as the equivalent cross-sectional area $\overline{A}$, the moment of inertia $\overline{I}_y$, $\overline{I}_z$, and the polar moment of inertia $\overline{J}$, defining the element that simulates the cracked component, are obtained through comparison of the equivalent stiffness matrix $[\overline{K}]$ with the stiffness matrix of the element with parameters $\overline{A}$, $\overline{I}_y$, $\overline{I}_z$, and $\overline{J}$:

$$\overline{A} = \frac{\overline{K}_{uu}L}{E}, \qquad \overline{I}_y = \min\left\{\frac{\overline{K}_{ww}L^3}{12E}, \frac{\overline{K}_{\theta_y\theta_y}L}{4E}\right\},$$

$$\overline{I}_z = \min\left\{\frac{\overline{K}_{vv}L^3}{12E}, \frac{\overline{K}_{\theta_z\theta_z}L}{4E}\right\}, \quad \text{and} \quad \overline{J} = \min\left\{\overline{I}_y + \overline{I}_z, \frac{\overline{K}_{\theta_x\theta_x}L}{G}\right\}$$

where $\overline{K}_{uu}$, $\overline{K}_{vv}$, $\overline{K}_{ww}$, $\overline{K}_{\theta_x\theta_x}$, $\overline{K}_{\theta_y\theta_y}$, and $\overline{K}_{\theta_z\theta_z}$ are the diagonal elements of matrix $[\overline{K}]$ corresponding respectively to the nodal displacements u_1, v_1, w_1, θ_{x1}, θ_{y1}, and θ_{z1}; L is the length of the cracked component.

4. Experimental and Numerical Validation

To verify the above theory, both lab tests and numerical calculations are conducted. The verification of the theory is to confirm the stiffness of the cracked beam as shown in Fig. 3, i.e., to compare the $P \sim V$ curve, where P is the load on the beam, and V is the corresponding displacement. The load P and deflection V are recorded simultaneously. The meshing of the cracked beam by FEM is demonstrated in Fig. 4. The results are summarized in Table 1, and presented in Fig. 5. It can be seen that the results from the derived theory are in good agreement with both the test data and numerical calculations.
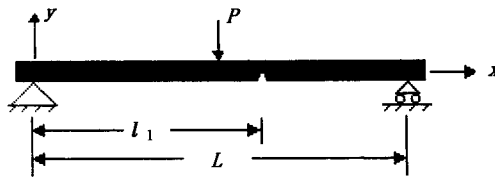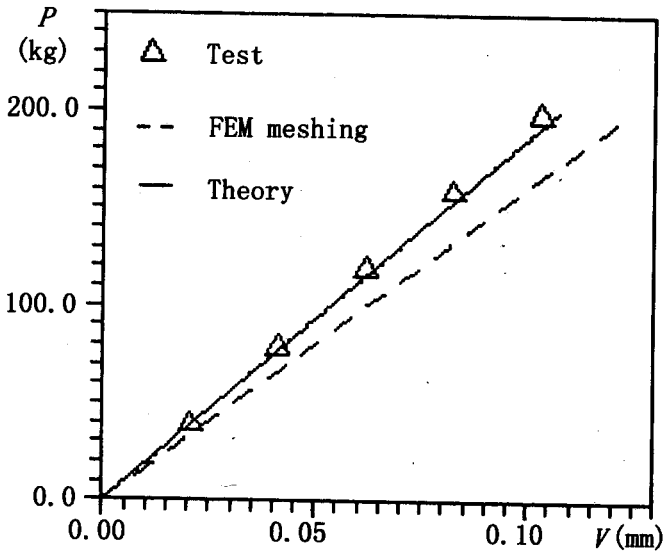

Fig. 3. Validation test on a cracked beam.

Fig. 4. Numerical validation by meshing the cracked beam ($l_1 = 14$ cm).

Table 1   Deflection at the central point of the cracked beam, mm ($l_1 = 14$ cm)

P (kg)		40	80	120	160	200
Theory	$a = 8$ mm	− 0.0179	− 0.0358	− 0.0537	− 0.0716	− 0.0895
FEM meshing	$a = 8$ mm	− 0.0195	− 0.0390	− 0.0585	− 0.0780	− 0.0975
Test	$a = 8$ mm	− 0.019	− 0.038	− 0.058	− 0.077	− 0.096

Fig. 5. $P \sim V$ curve for the cracked beam ($l_1 = 14$ cm).

## 5. Application to Assessment of Safety of Cracked Platforms

A subroutine program named DASA is written for the application of the above theory to the FE calculation of steel structures with ABAQUS. A fixed platform and a self-elevating jack-up drilling rig are simulated for the analysis.

5.1 Fixed Platform

The fixed platform operating in the Bohai Gulf is simplified as shown in Fig. 6 for the application of the derived theory. The diameter and thickness of the jacket leg are 0.99 m and 0.025 m respectively; the brace's diameter and thickness are 0.529 m and 0.007 m. For simplicity, it is supposed that only a horizontal force of 1000 kN and a vertical load of 500 kN are acting on the platform. A crack of 16 cm in length occurs in element 35 with node number 33 and 44. The effective parameters of the cracked element are calculated according to the present theory, as presented in Table 2. The displacements of the fixed platform with or without cracks are presented in Table 3. The maximum axial stresses in the structure are summarized in Table 4. It can be seen that the effect of the crack on the fixed platform is quite prominent.

Table 2   Parameters of element 35

	$A(m^2)$	$I_y(m^4)$	$I_z(m^4)$	$J_\rho(m^4)$
Without crack	0.75791E – 1	0.88282E – 2	0.88282E – 2	0.17656E – 1
Cracked	0.75773E – 1	0.88282E – 2	0.84336E – 2	0.17262E – 1
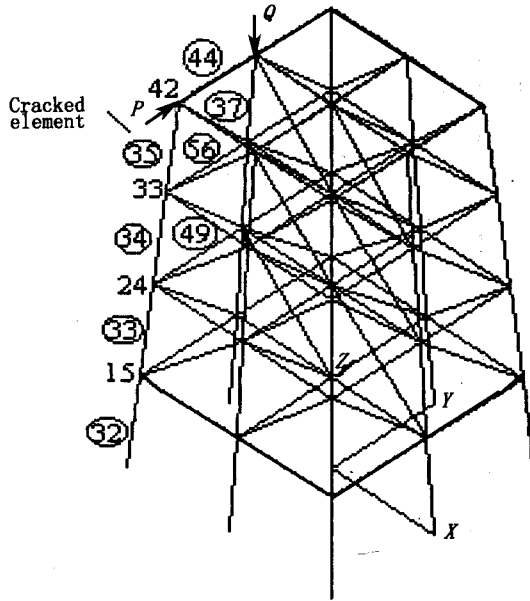
Fig. 6. Structure of a simplified fixed platform.

Table 3   Effect of crack on the displacement of the fixed platform

Node No.		x	y	z	θ_x	θ_y	θ_z
Without crack	15	– 24.77	70.72	– 1.706	– 0.0947	– 3.358E – 2	– 0.0782
	24	– 25.79	75.60	– 0.7272	0.0122	– 1.175E – 4	– 0.1008
	33	– 25.42	81.33	– 0.1682	– 0.0207	– 2.329E – 3	– 0.1152
	42	– 23.80	90.01	– 0.2035	– 0.0147	4.774E – 5	– 0.1364
Cracked	15	– 27.63	78.46	– 1.862	– 0.1078	– 3.741E – 2	– 0.0866
	24	– 28.76	83.77	– 0.7474	0.0179	– 7.205E – 5	– 0.1126
	33	– 28.33	90.76	– 0.1279	– 0.0142	– 2.528E – 3	– 0.1242
	42	– 26.45	99.44	– 0.1896	– 0.0099	2.096E – 4	– 0.1423

## 5.2 Self-Elevating Drilling Rig

Cracks are discovered in self-elevating drilling rigs whenever MT inspection is conducted. The focus of this part is on the strength of the legs having cracks, and the hull structure is simulated as simply as possible. Fig. 7 shows the FE model of the rig.

Table 4   Maximum axial stresses in the structure σ_{xmax}, MPa

| Element No.	Without crack	Cracked
32	136.05	141.91
33	43.82	45.50
34	20.91	20.82
35	17.74	19.15
37	27.55	28.35
44	−29.52	−29.32
49	15.21	16.06
56	24.94	28.17
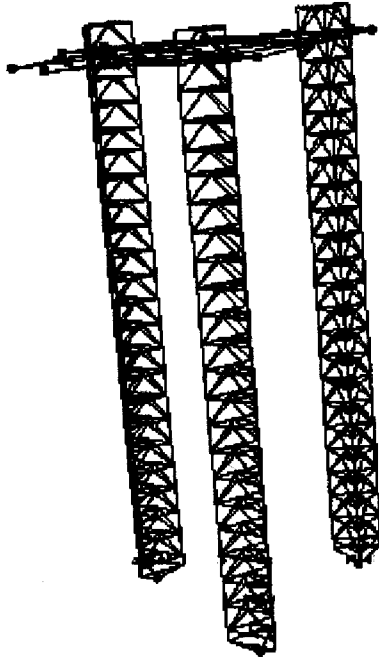
Fig. 7. FE model of the drilling rig.

It is assumed that a crack occurs in the interaction between the pile of the leg and the spud-can. The parameters of the crack as illustrated in Fig. 8 are as follows: $\bar{A} = 0.109 \text{ m}^2$, $\bar{I}_y = 12.59 \times 10^{-3}$ m^4, $\bar{I}_z = 2.71 \times 10^{-3} \text{ m}^4$, and $J = 2.78 \times 10^{-3} \text{m}^4$. The results are presented in Table 5 where the elements numbered are located in the interaction between the pile of the leg and the spud-can. It can be seen that for such kind of rigs, one crack has little effect on the stress state of the structure, not endangering the safety of the rig. It can be explained that the three legs have very strong support to the strength of the rig which is hyperstatic, and even a loss of a brace will not affect the safety of the rig.

The compressive stress state as shown in Table 5 is also a contribution to the inaction of the crack on the strength of the rig.

Table 5   Effect of the crack on the stresses of the drilling rig, Pa

Element No.	Without crack	Cracked
102	$-0.684560E+08$	$-0.684590E+08$
103	$-0.648460E+08$	$-0.649160E+08$
104	$-0.612630E+08$	$-0.612650E+08$
105	$-0.565280E+08$	$-0.565380E+08$
106	$-0.634020E+08$	$-0.634710E+08$
107	$-0.573050E+08$	$-0.573100E+08$
174	$-0.585300E+08$	$-0.585380E+08$
176	$-0.584040E+08$	$-0.584090E+08$
177	$-0.483320E+08$	$-0.483250E+08$
180	$-0.439320E+08$	$-0.439450E+08$
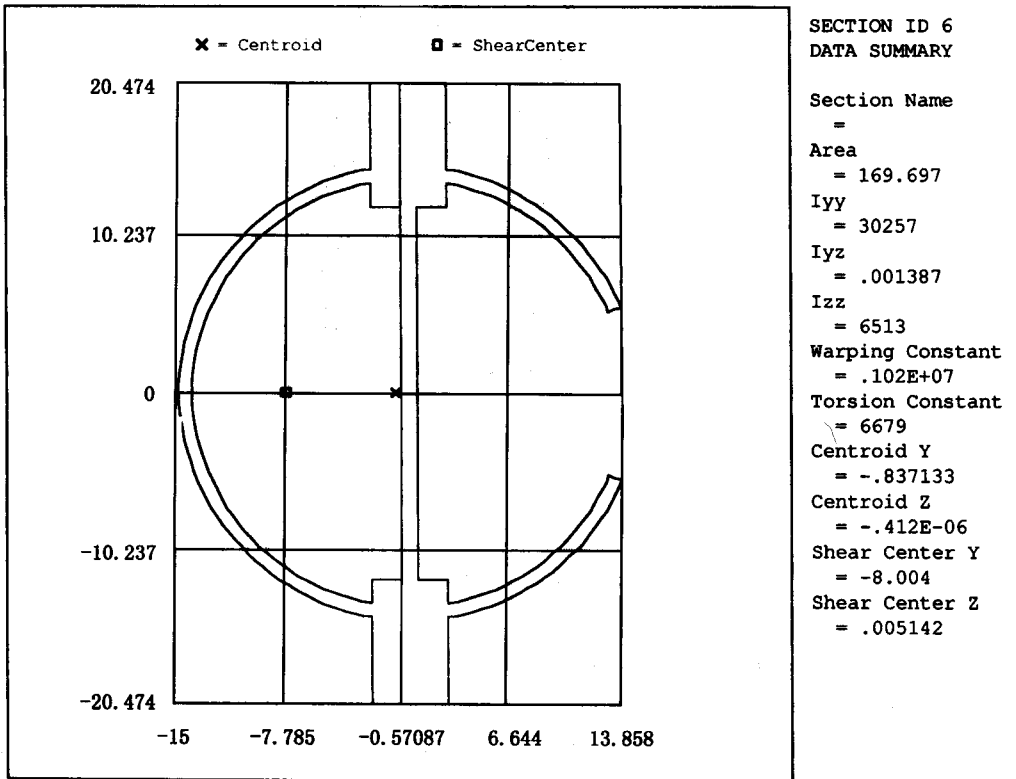
Fig. 8. Cracking of the pile of the rig leg.

6. Conclusions

(1) On the basis of the finite variation principle, static condensation method and fracture mechanics, a finite element method is developed to calculate the stiffness matrix of the cracked component. The equivalent parameters such as the equivalent cross-sectional area $\bar{A}$, the moment of inertia $\bar{I}_y$, $\bar{I}_z$, and the polar moment of inertia $\bar{J}$, which define the element simulating the cracked component for the FE model of the structure, are mathematically expressed. The theories proposed in this paper are validated by means of both laboratory tests and numerical calculations. They can be a basis for the application of the FE structural analysis software to the calculation of large scale steel structures containing cracks.

(2) As an application of the theory, a subroutine program named DASA is written and incorporated into ABAQUS. A fixed production platform is simplified and a self-elevating jack-up drilling rig is modeled for evaluation of the effect of cracks on the strength of the structures, and the results indicate that one crack has little effect on the stress state of such structures as rigs due to their hyperstaticity while the effect of cracks on the fixed platform is prominent.

References

Duan M. L. and Liu C. T., 1995. Investigation on failure of offshore steel structures under sea ice conditions, *Proceedings of the Int. Conference on Technologies for Marine Environment Preservation* (MARIENV'95), Tokyo, Japan, Sep. 24 – 29, 1995, Vol.1, 71 ~ 74.

Duan M. L. and Qin T. Y., 1999. *Damage assessment on the integrity of drilling rigs*, Technical report, China Classification Society, Sept., 1999. (in Chinese)

Gudmundson, P., 1982. Eigenfrequency changes of structures due to cracks, notches or other geometrical changes, *J. Mech. Phys. Solids*, **30**(5): 339 ~ 353.

Irwin, G. R. and Kies, J. A., 1954. Critical energy rate analysis of fracture strength of large welded structures, *Welding Journal*, **33**, 1935 ~ 1985.

Liu C. T., Qin T. Y. and Duan M. L., 2002. Finite element analysis of damaged legs of offshore platform structures, *China Ocean Engineering*, **16**(3): 311 ~ 320.

Lubahn, J. D., 1959. Experimental determination of energy release rate for notch bending and notch tension, *Proc. ASTM*, **58**, 885 ~ 915.

Qian, G. L., Gu, S. N. and Jiang, J. S., 1990. The dynamic behavior and crack detection of a beam with a crack, *Journal of Sound and Vibration*, **138**(2): 233 ~ 243.

Ricles, J. M., Bruin, W. M. and Sooi, T. K., 1994. Residual strength and repair of dent-damaged tubulars and the implication on offshore platform reassessment and requalification, 1994 *OMAE*, Vol. 2, 179 ~ 189.